Physicochem. Probl. Miner. Process., 54(2), 2018, 270-277

http://www.journalssystem.com/ppmp

Physicochemical Problems of Mineral Processing

ISSN 1643-1049

Received March 11, 2017; reviewed; accepted June 09, 2017

Efficient sulfidization of lead oxide at high temperature using pyrite as vulcanizing reagent

Yong-Xing Zheng [1,2], Jin-Fang Lv [1,3], Hua Wang [1,2], Shu-Ming Wen [1], Lingyun Huang [1]

[1] Kunming University of Science and Technology, State Key Laboratory of Complex Nonferrous Metal Resources Clean Utilization, Kunming 650093, China

[2] Kunming University of Science and Technology, Faculty of Metallurgical and Energy Engineering, Kunming 650093, China

[3] Kunming University of Science and Technology, Faculty of Land Resource Engineering, Kunming 650093, China

Corresponding author: jflv2017@126.com (Lv Jin-Fang)

Abstract: A sulfidization roasting-flotation process was usually viewed to be effective in treating the refractory oxide ore. In this paper, pyrite was proposed to be applied as a potential vulcanizing reagent to transform PbO or its surface to PbS based on feasibilities of technology and economy. The evolution process, phase and characteristics of crystal growth were investigated by TG, XRD and SEM-EDS, respectively, to interpret the interaction mechanism of lead oxide and pyrite at high temperature. It was found that the decomposition process of pyrite under argon atmosphere was a slow process of sulfur released from FeS_2 to Fe_xS, which made the process easier to be controlled. When PbO was introduced into the system, the initial solid-solid (PbO-FeS_2) reaction and prevailing solid-gas (PbO-S_2(g)) reaction occurred at about 500 °C and 700 °C, respectively. Combined with the SEM-EDS analyses results, the optimal temperature for the sulfidization of PbO should be in the range of 700-750 °C.

Keywords: *lead oxide, sulfidization roasting, pyrite, reaction mechanism, TG*

1. Introduction

Lead is extensively applied to various industrials such as battery manufacture, building, electronics, etc. Statistically, more than 80% of lead is produced from lead sulfide concentrates by conventional oxidization-reduction smelting processes in the world (Zheng et al., 2015a; Peng et al., 2003). With the exploitation of resources, the primary resources are soon going to be insufficient to supply the demand. The lead oxide ores may become the significant source to offer the above metals. However, it seems to be difficult for valuable metal recovery from the refractory ores characterized by complex composition and high content of slime (Lan et al., 2013). Lead is mainly in the form of carbonates in the oxide ores and in the past years, many technologies such as flotation or flotation combined with gravity separation, hydrometallurgy and pyrometallurgy have been tested for treating the refractory ores, in which a sulfidization-xanthate flotation method has been the most commonly and commercially applied for the concentration of lead oxide minerals.

Sodium sulfide is one of the most widely used alkali metal sulfides for converting the surface of oxide minerals or metal ions in the solution into sulfides (Mehdilo et al., 2013; Dai et al., 2015). The sulfidized lead oxide mineral can be well recovered with xanthate due to the similar nature of natural galena (Sun et al., 2016; Ejtemaei et al., 2014). Thus, sulfidization is the most critical stage for the sulfidization-xanthate flotation method. However, its effectiveness is not entirely satisfactory due to the fact that the sulfidized layer detaches readily (Park et al., 2016; Liu et al., 2015). If an effective method to sulfidize the lead oxide mineral is developed, the existing mineral processing methods can be applied to treat these pre-treated oxides.

http://dx.doi.org/10.5277/ppmp1813

Recently, the transformation of oxides or their surfaces to sulfides has received considerable attentions. A mechanical-chemical process was reported to treat the lead oxide by grinding with sulfur and iron powders at a room temperature (Tan et al., 2015; Yuan et al., 2012), but the flotation concentrate always gave a poor recovery due to the artificial sulfides characterized by fine crystallization. Hydrothermal sulfidization was also suggested to treat the lead oxide, but it seemed to be difficult in practice due to the slow transformation process (Li et al., 2012; Liang et al., 2012). Generally, higher temperature is favorable for improving the reaction rate (Zheng et al., 2014; Han et al., 2016a; Zheng et al., 2016; Lv et al., 2017), and therefore the roasting process was proposed. Li et al. (2010) investigated the sulfidization roasting of a low grade lead-zinc oxide ore with elemental sulfur and the sulfidization extent of Pb could reach 98%. Under this condition, a lead recovery of 79.5% was obtained after flotation. However, the process needed to be performed in an airtight device due to the easier volatilization nature of elemental sulfur. In order to improve the roasting process, Zheng et al. (2015b) adopted a method of temperature gradient for transforming lead carbonate into lead sulfide and a lead sulfidization extent of 96.50% was obtained. Nevertheless, the roasting process was rather difficult to be controlled.

Compared with the elemental sulfur, pyrite seems to be potential in practical operation attributed to a low cost and the slow release of sulfur from the crystal lattice, which made the process easier to be controlled. Previous studies mainly focused on the synthesis (Xiao et al., 2016; Golsheikh et al., 2013) and thermal decomposition (Li et al., 2015) of pyrite, but there was little work reported about transformation of PbO or its surface to PbS with pyrite at high temperature. In this paper, the evolution process, phase and characteristics of crystal growth were investigated by thermogravimetry (TG), XRD and SEM-EDS, respectively, to interpret the reaction mechanism. The goal was to reveal the interaction between PbO and pyrite at high temperature and make the sulfidization roasting process feasible technologically and economically.

2. Materials and methods

2.1 Materials

XRD pattern of PbO is shown in Fig. 1, which reveals the sample with a high purity. The PbO sample was prepared by decomposing basic lead carbonate ($(PbCO_3)_2 \cdot Pb(OH)_2$) with an analytical grade at 600 °C. Pyrite containing 47% Fe and 47.9% S was used as a vulcanizing reagent and its XRD pattern is presented in Fig. 2, which also indicates the sample with a high purity. Argon (Ar) was used as a protective gas with a purity of 99.999%.

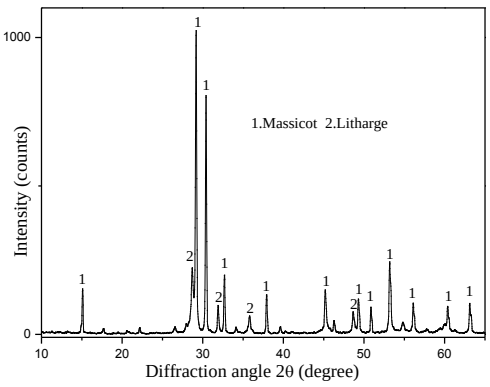

Fig. 1. XRD pattern of synthesized PbO

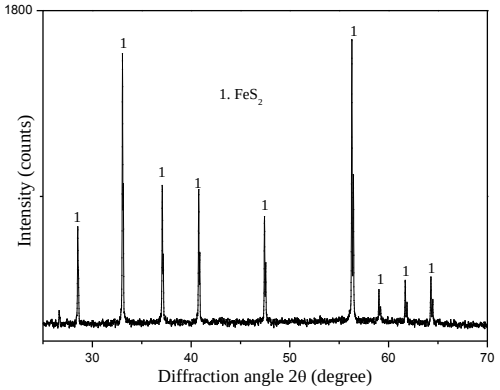

Fig. 2. XRD pattern of pyrite

2.2 TG tests

Roasting of lead oxide with pyrite was conducted using a thermalanalyser (NETZSCH5, STA 449 F3) equipped with a computer, where some parameters such as initial and final temperature, gas flow rate, sample mass and heating rate could be exactly preset. Firstly, the pyrite and lead oxide was respectively weighted using an electronic balance with an accuracy of 1×10^{-4} g, and then were mixed, placed on a pan of Al_2O_3, and suspended on the holder. A vertical electric furnace tube was moved

downward, and a vacuum of 99% was generated. With the flow of argon from the bottom of the furnace at a rate of 100 cm^3/min, the vacuum was slowly released to zero. The non-isothermal tests were carried out within 900 °C at a heating rate of 10-20 K/min. In the isothermal tests, sample was heated at a heating rate of 30 K/min to a desired temperature, and then reacted for 120 min. The reactions during the roasting may be described as (Hu et al., 2006):

$$FeS_2 = FeS + 1/2S_2(g)\,, \tag{1}$$

$$2/3PbO + FeS_2 = 2/3PbS + FeS + 1/3SO_2(g)\,. \tag{2}$$

From Eqs. (1) and (2), it can be known that 1 mole of elemental sulfur will be lost when 1 mole of FeS_2 was heated (Eq. (1)). Only 1/3 mole of sulfur in the form of SO_2 will be lost when the PbO was added into the system. Therefore, the amount of pyrite (M=30.0 mg) was fixed, while the amount of PbO was varied to investigate the interaction between PbO and FeS_2 in the non-isothermal process.

2.3 XRD and SEM-EDS analyses

The samples obtained from the isothermal tests were examined on a Germany Bruker-axs D8 Advance X-ray powder diffractometer (XRD) with Cu Kα radiation (λ = 1.5406 Å). The operation voltage and current were kept at 40 kV and 40 mA, respectively. Surface morphological analyses of the products obtained were detected by SEM. The SEM (JEOL.LTD, JSM-6360LV) was working at 20 kV electron accelerating voltage. Semiquantitative information analyses were also performed using an X-ray energy dispersive spectrometer (EDAX.LTD, EDX-GENESIS 60S) coupled with the SEM.

3. Results and discussion

3.1 Non-isothermal thermogravimetric tests

As mentioned before, the decomposition of pyrite and sulfidization of PbO simultaneously occurred during the whole reaction. Therefore, it was necessary to firstly investigate the thermal decomposition behavior of pyrite, as shown in Fig. 3. From Fig. 3(a), it can be seen that the sample mass slightly decreased when temperature increased from 480 to 550 °C. This may be accounted by the oxidization reaction between pyrite and oxygen adsorbed (Eq. (5)) (Li et al., 2005):

$$3FeS_2 + 8O_2(g) = Fe_3O_4 + 6SO_2(g)\,. \tag{5}$$

The sample mass was slightly fluctuated as temperature increased from 550 °C to 580 °C, which revealed that the oxygen adsorbed had already been consumed at about 550 °C. Mass loss continued and their maximum rates appeared at about 680 °C when the temperature increased to 700 °C. This could be explained as (Hu et al., 2006; Lv et al., 2015):

$$FeS_2(s) = FeS_x(s) + (1 - 0.5x)S_2(g)\,, \tag{6}$$

$$Fe_3O_4 + 5/2S_2(g) = 3FeS + 2SO_2(g)\,. \tag{7}$$

With further increasing temperature, the sample mass slightly decreased, indicating that the decomposition of pyrrhotine (FeS_x) continuously occurred (Hu et al., 2006):

$$FeS_x(s) = FeS(s) + 0.5(x - 1)S_2(g)\,. \tag{8}$$

These results indicated that the decomposition process of pyrite under argon atmosphere was a slow process of sulfur released.

In addition, the DTG curves, as presented in Fig. 3(b), show that the mass loss rate increased with increasing heating rate and the rate extremum appeared at 680 °C. It was known that faster or slower decomposition of pyrite would not be favorable for the sulfidization of PbO. So the intermediate value (15 K/min) of heating rate was selected and the subsequent non-isothermal thermogravimetric tests were carried out at this condition.

Fig. 4 shows the TG curves with respect to temperature and different molar ratio of FeS_2 to PbO. It can be seen that the sample mass was slightly fluctuated and then began to decrease until the temperature increased to about 500 °C. This could be explained as follow:

$$9/2FeS_2 + 8PbO = 8PbS + 3/2Fe_3O_4 + SO_2(g) \quad \Delta G_T^{\theta} = -495.4\text{kJ}, T = 298\text{K}\,. \tag{9}$$

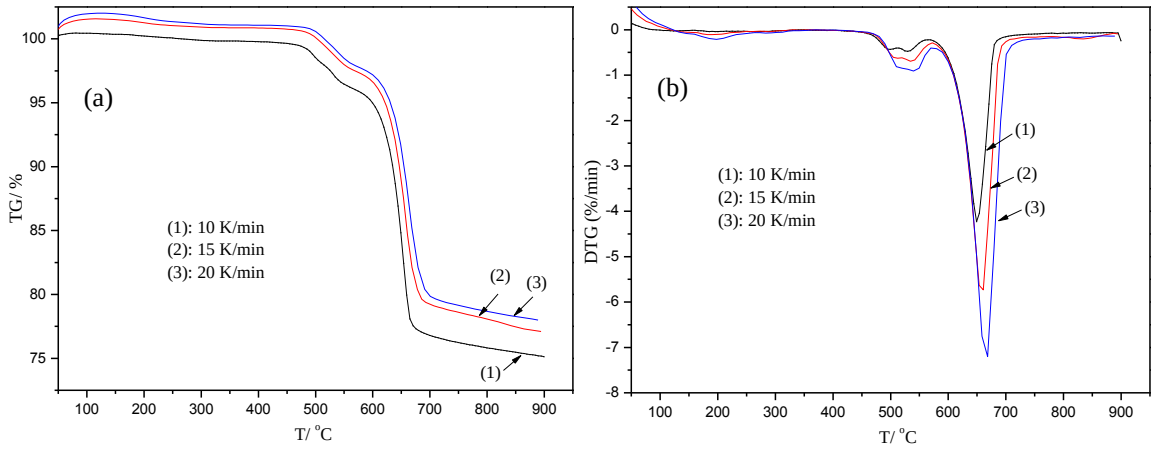

Fig. 3. TG and DTG curves of pyrite at different heating rate

Mass loss continued when temperature increased to 700 °C, which could be explained by the decomposition of pyrite (Eq. (7)). In addition, it was found that remaining percentage of the sample increased with increasing the amount of PbO, confirming that the solid-gas reaction indeed occurred as follow (Zheng et al., 2015b):

$$2PbO(s) + 3/2S_2(g) = 2PbS(s) + SO_2(g) \quad . \tag{10}$$

Surprisingly, mass loss of the sample still continued when the temperature increased above 700 °C, especially for the sample containing significant amounts of PbO (n_{Fes2}:n_{PbO}=1~1.5). This could be attributed to the further decomposition of pyrrhotine (FeS_x) (Eq. (8)) and the interaction between PbO and PbS generated:

$$2PbO(s) + PbS = 3Pb(l) + SO_2(g) \quad . \tag{11}$$

The latter was dominant for the mass loss especially when temperature increased to 800 °C (Zheng et al. 2015c). Therefore, the preferable temperature for the sulfidization of PbO was determined to be about 700 °C.

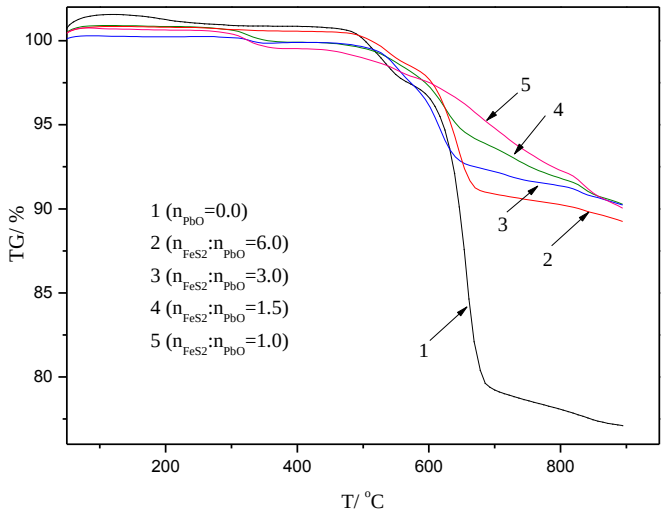

Fig. 4. TG curves of samples with respect to temperature and different molar ratio of FeS_2 to PbO

3.2 Isothermal TG tests and analyses of phase and morphology

In order to further confirm the above deduction, isothermal TG tests and analyses of phase and surface morphology were carried out, and the results are shown in Figs. 5-7. From Fig. 5, it can be seen that the mass loss sharply decreased in the time range of 10-25 min. Combined with the TG curves in

Fig. 4, it can be known that the mass loss was mainly attributed to the solid-gas reaction (Eq. (10)) and decomposition of pyrite (Eq. (6)). In addition, it can be seen that the remaining percentage of the sample decreased with the increase in temperature, which was ascribed to the fact that the higher the temperature was, the faster the decomposition of pyrite would be.

Fig. 6 shows the XRD patterns of the roasted products and it can be seen that there were obvious peaks of PbS, weak peaks of Fe_xS, $Fe_{2.964}O_4$ and PbO at 550 °C, indicating that the reactions involving Eqs. (9) and (10) occurred. The peak of PbO disappeared when the temperature increased to 650 °C. With further increasing temperature, there was no obvious change for the peaks. All of these results were consistent with the non-isothermal and isothermal thermogravimetric tests.

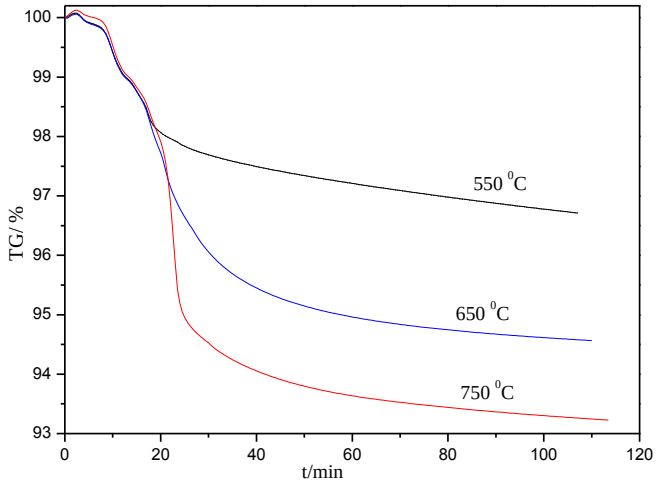

Fig. 5. TG curves of the sample with respect to time and temperature (n_{Fes2}:n_{PbO}=1:1)

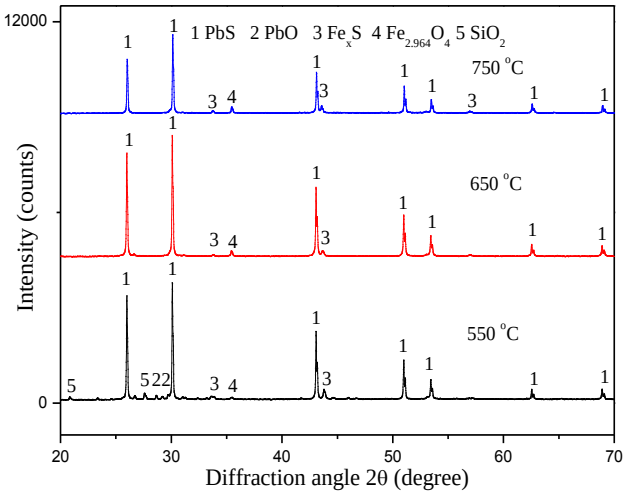

Fig.6. XRD patterns of roasted products at different temperature

Fig. 7 presents the BSE images and EDS spectrums of the obtained samples at different temperature. It can be observed that significant amounts of PbS were formed at 550 °C., however the generated ones occurred as irregular particles at an average size of 1 μm. The obtained PbS particles existed as aggregation when the temperature increased to 650 °C. With further increasing temperature, the generated ones occurred as regular crystals with shapes of tetrahedron and octahedron at an average size of 10 μm, which would be favorable for the following flotation (Han et al., 2016b, 2017a; 2017b). These results indicated that temperature played a key role in controlling the growth of PbS crystal. Therefore, the optimal temperature for the sulfidization of PbO should be in the range of 700-750 °C.

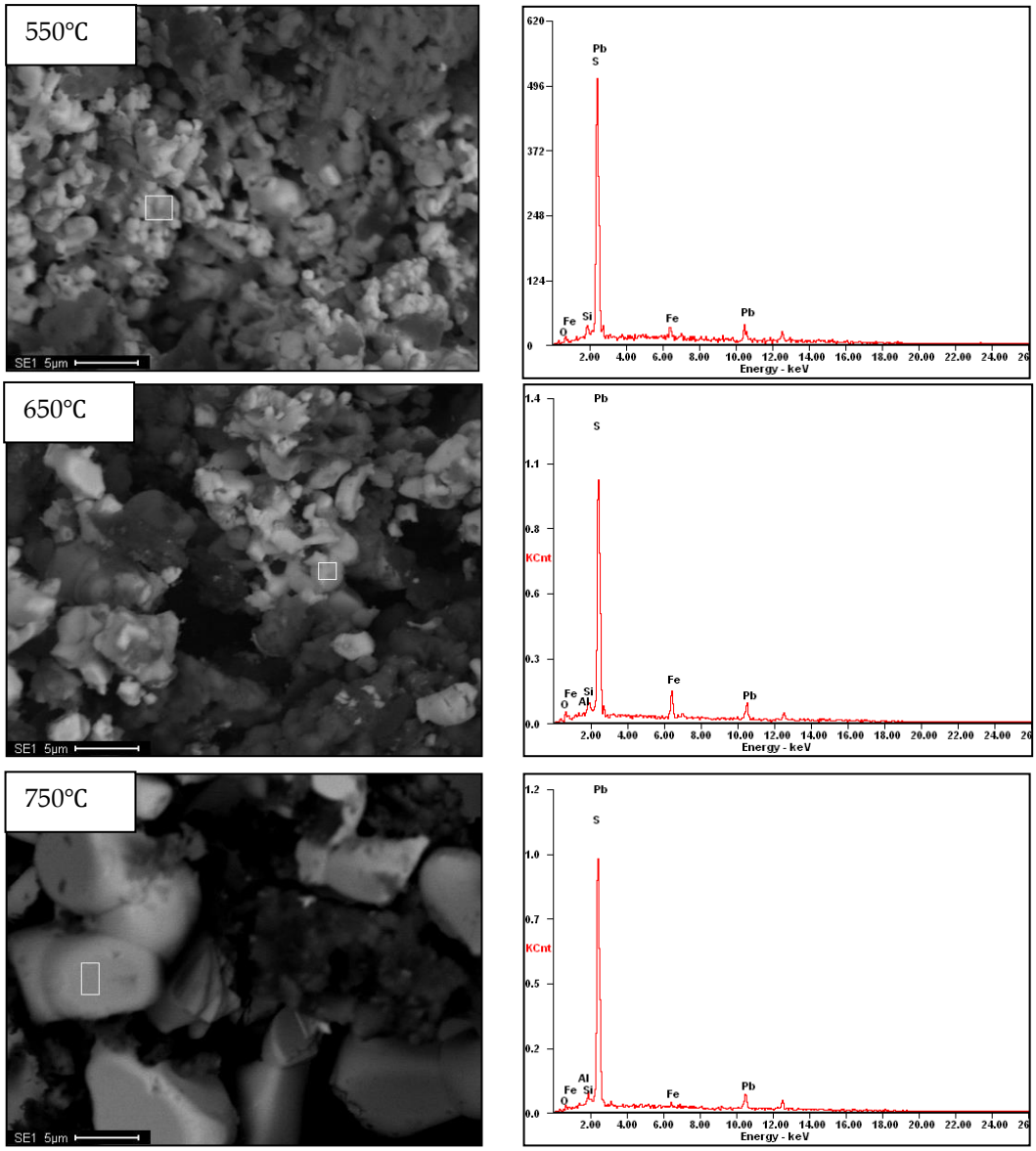

Fig. 7. BSE images and EDS spectrums of roasted products at different temperatures

4. Conclusions

Pyrite was proposed to be used as a potential vulcanizing agent to transform PbO or its surface to PbS and the reaction mechanism was investigated. It was found that the decomposition process of pyrite under argon atmosphere was a slow process of sulfur released from FeS_2 to Fe_xS. When the PbO was introduced into the system, the initial solid-solid (PbO-FeS_2) reaction and prevailing solid-gas (PbO-S_2(g)) reaction occurred at about 500 °C and 700 °C, respectively. The generated PbS occurred as regular crystals at an average size of 10 μm at 750 °C., which would be favorable for following flotation. In practice, only small amount of pyrite was added to transform the surface of PbO into PbS, which could be well recovered by a conventional flotation process. These findings could provide a theoretical support for improving the sulfidization roasting process of lead oxide ore and other nonferrous metal oxides materials.

Acknowledgements

The authors would like to acknowledge the National Natural Science Foundation of China (No. 51604131), the Yunnan Province Applied Basic Research Project (2017FB084), the Yunnan Province Collaborative Innovation

Center Fund of Complex Nonferrous Metal Resources Comprehensive Utilization (KKPT201663011), the Talent & Training Program of Yunnan Province (No. KKSY201563041) and the Testing and Analyzing Funds of Kunming University of Science and Technology (No. 2016T20150055, No. 2016P2013101003 and No. 2017T20090159) for financial support.

References

DAI J., YANG X., HAMON M., KONG L., 2015. *Particle size controlled synthesis of CdS nanoparticles on a microfluidic chip*. Chemical Engineering Journal, 280(5), 385-390.

EJTEMAEI M., GHARABAGHI M., IRANNAJAD M., 2014. *A review of zinc oxide mineral beneficiation using flotation method*. Advances in Colloid and Interface Science, 206(2), 68-78.

GOLSHEIKH A M., HUANG N M., LIM H N., CHIA C H., HARRISON I., MUHAMAD M R., 2013. *One-pot hydrothermal synthesis and characterization of FeS_2 (pyrite)/graphene nanocomposite*. Journal of Chemical engineering, 218(3), 276-284.

HAN J W., LIU W., WANG D W., JIAO F., QIN W Q., 2016a. *Selective sulfidation of lead smelter salg with sulfur*. Metallurgical and Materials Transactions B, 47(1), 344-354.

HAN J W., LIU W., WANG D W., JIAO F., ZHANG T F., QIN W Q., 2016b. *Selective Sulfidation of Lead Smelter Slag with Pyrite and Flotation Behavior of Synthetic ZnS*. Metallurgical and Materials Transactions B, 47, 2400-2410.

HAN J W., LIU W., ZHANG T F., XUE K., LI W H., JIAO F., QIN W Q., 2017a. *Mechanism study on the sulfidation of ZnO with sulfur and iron oxide at high temperature*. Scientific Reports 7, 42536.

HAN J W., LIU W., QIN W Q., ZHANG T F., CHANG Z Y., XUE K., 2017b. *Effects of sodium salts on the sulfidation of lead smelting slag*. Minerals Engineering, 108, 1-11.

HU G., DAM-JOHANSEN-DAM., WEDEL S., HANSEN J P., 2006. *Decomposition and oxidation of pyrite*. Progress in Energy and Combustion Science, 32(2), 295-314.

LAN Z Y., LI D., LIU Q., TONG X., 2013. *Study on Flotation of Lead-zinc Oxide Ore from Yunnan*. Environmental Protection and Resources Exploitation, 1(3), 2317-2322.

LIU W., WEI D Z., MI J., SHEN Y., CUI B., HAN C., 2015. *Immobilization of Cu(II) and Zn(II) in simulated polluted soil using sulfurizing agent*. Chemical Engineering Journal, 277(2), 312-317.

LI C X., WEI C., SONG Y., DENG Z G., LIAO J Q., XU H S., LI M T., LI X B., 2012. *Hydrothermal sulfidation of white lead with elemental sulfur*. Advanve in chemical engineering, 624-630.

LIANG Y J., CHAI L Y., LIU H., MIN X B., MAHMOOD Q., ZHANG H J., KE Y., 2012. *Hydrothermal sulfidation of zinc-containing neutralization sludge for zinc recovery and stabilization*. Mineral Engineering, 25(5), 14-19.

LI H Y., ZHANG S H., 2005. *Detection of mineralogical changes in pyrite using measurements of temperature-dependence susceptibilities*. Journal of geophys, 48(5), 1384-1391.

LI Y., WANG J K., WEI C., LIU C X., JIANG J B., WANG F., 2010. *Sulfidation roasting of low grade lead-zinc oxide ore with elemental sulfur*. Mineral Engineering, 23, 563-566.

LV W., YU D., WU J., ZHANG L., XU M., 2015. *The chemical role of CO_2 in pyrite thermal decomposition*. Proceedings of the Combustion Institute, 35 (2), 3637-3644.

LV J F., ZHANG H P., TONG X., FAN C L., YANG W T., ZHENG Y X., 2017. *Innovative methodology for recovering titanium and chromium from a raw ilmenite concentrate by magnetic separation after modifying magnetic properties*. Journal of Hazardous Materials, 325, 251-260.

MEHDILO M., IRANNAJAD M., ZAREI H., 2013. *Flotation of zinc ore using cationic and cationic-anionic mixed collectors*. Physicochemical Problems of Mineral Processing, 49 (2), 145-156.

PARK J., PARK S., CHOI J., KIM G., TONG M P., KIM H., 2016. *Influence of excess sulfide ions on the malachite-bubble interaction in the presence of thiol-collector*. Separation and purification technology, 168(2), 1-7.

PENG R Q., REN H J., ZHANG X., 2003. *Metallurgy of lead and zinc*. Beijing: Science Press.

SUN W., SUN C., LIU R Q., CAO X F., TAO H B., 2016. *Electrochemical behavior of galena and jamesonite flotation in high alkaline pulp*. Transactions of Nonferrous Metals Society of China, 26(1), 551-556.

TAN Q Y., LI J H., 2015. *Recycling Metals from Wastes: A Novel Application of Mechanochemistry*. Environment Science Technology, 49(2), 5849-5861.

XIAO S., LI X., SUN W., GUAN B., WANG Y., 2016. *General and facile synthesis of metal sulfide nanostructures: In situ microwave synthesis and application as binder-free cathode for Li-ion batteries*. Chemical Engineering, 306(2), 251-259.

YUAN W Y., LI J H., ZHANG Q W., SAITO F., 2012. *Mechanochemical sulfidization of lead oxides by grinding with sulfur*. Powder Technology, 230(1), 63-66.

ZHENG Y X., LIU W., QIN W Q., KONG Y., LUO H L., HAN J W., 2014. *Mineralogical Reconstruction of Lead Smelter Slag for Zinc Recovery*. Separation science and technology, 49(5), 783-791.

ZHENG Y X., LV J F., LIU W., QIN W Q., WEN S M., 2016. *An inonovative technology for recovery of zinc, lead and silver from zinc leaching residue*. Physicochemical Problems of Mineral Processing, 52(2): 943-954.

ZHENG Y X., LIU W., QIN W Q., HAN J W., YANG K., LUO H L., WANG D W., 2015a. *Improvement for sulphidation roasting and its application to treat lead smelter slag and zinc recovery*. Canadian Metallurgical Quarterly, 54 (1), 92-100.

ZHENG Y X., LIU W., QIN W Q., JIAO F., HAN J W., YANG K., LUO H L., 2015b. *Sulfidation roasting of lead and zinc carbonate with sulphur by temperature gradient method*. Journal of Central South University, 22(5), 1635-1642.

ZHENG Y X., LIU W., QIN W Q., HAN J W., YANG K., LUO H L., 2015c. *Selective reduction of $PbSO_4$ to PbS with carbon and flotation treatment of synthetic galena*. Physicochemical Problems of Mineral Processing, 51(2), 51.